FULL PAPER *Anatomy*

Canine Hippocampal Formation Composited into Three-Dimensional Structure Using MPRAGE

Mi-Ae JUNG[1)]**, Sang-Soep NAHM[2)]**, Min-Su LEE[1)], In-Hye LEE[1)], Ah-Ra LEE[1)], Dong-Pyo JANG[3)], Young-Bo KIM[3)], Zang-Hee CHO[3)] and Ki-Dong EOM[1)]*

[1)]Department of Veterinary Radiology and Diagnostic Imaging, [2)] Department of Veterinary Anatomy, College of Veterinary Medicine, Konkuk University, 1 Hwayang-dong, Kwangjin-ku, Seoul 143–701 and [3)]Neuroscience Research Institute, Gachon University of Medicine and Science, Incheon 405–760, Korea

(Received 11 November 2009/Accepted 10 February 2010/Published online in J-STAGE 24 February 2010)

ABSTRACT. This study was performed to anatomically illustrate the living canine hippocampal formation in three-dimensions (3D), and to evaluate its relationship to surrounding brain structures. Three normal beagle dogs were scanned on a MR scanner with inversion recovery segmented 3D gradient echo sequence (known as MP-RAGE: Magnetization Prepared Rapid Gradient Echo). The MRI data was manually segmented and reconstructed into a 3D model using the 3D slicer software tool. From the 3D model, the spatial relationships between hippocampal formation and surrounding structures were evaluated. With the increased spatial resolution and contrast of the MPRAGE, the canine hippocampal formation was easily depicted. The reconstructed 3D image allows easy understanding of the hippocampal contour and demonstrates the structural relationship of the hippocampal formation to surrounding structures *in vivo*.
KEY WORDS: 3D, canine, hippocampal formation, MPRAGE.

J. Vet. Med. Sci. 72(7): 853–860, 2010

The hippocampal formation is located in the medial surface of the temporal lobe, along the floor and medial wall of the temporal horn of the lateral ventricle [1, 2]. The hippocampal formation is shaped like a C [19]. It extends in a curve, starting from the amygdala ventrally in each piriform lobe and progressing caudodorsally and then cranially over the diencephalon [8, 21]. The caudal end of the hippocampal formation tapers under the splenium of the corpus callosum [22]. Dorsal to the caudal thalamus, the hippocampal formation of each cerebral hemisphere meets at the medial plane, and the fornix, the hippocampal commissure, is formed at this region [2, 8]. The hippocampal formation can be divided into three parts: a cranial part, or head, a middle part, or body and a caudal part, or tail [8]. It is again divided into 3 main transverse zones: the dentate gyrus; the hippocampal proper, also called the cornus ammonis (CA); and the subiculum [1, 2, 24].

Abnormalities of the hippocampal contour and volume play important roles in several functions such as spatial response in dogs [12] and disease including Alzheimer-type dementia [5], depression [18], or schizophrenia [17] in human. Structural change of the hippocampal formation has been presented on MR images (MRI) [5, 17]. These have been resulted in increased importance of the precise understanding of the hippocampal anatomy. These also have made three-dimensional (3D) hippocampal structure importance in medical image.

MRI has been the principal method for studying structural brain change *in vivo* [11]. Normal MR images of canine brain has been described in previous studies [13, 14]. They have only depicted the normal canine brain using a low field strength MRI scanner. In those images, description of the hippocampal formation and the perihippocampal structures were not available. It was because of their small size and ambiguity with the perihippocampal structures and low field strength having decreased signal to noise ratio [11].

There haven't been MRI studies that focused on the hippocampal formation itself. In addition, it is not easy to comprehend 3D relationship among the brain structures on MRI. Currently, the 3D canine hippocampal image is not available. Previously reported data only revealed the limited surface of the canine hippocampal formation in two-dimensional (2D) image such that it was not able to fully articulate relationships of the hippocampal formation to surrounding cerebral structures [13, 14, 21].

There has been no *in vivo* canine hippocampal formation reconstructed in 3D structure. The aim of the present study is to perform MPRAGE and aquire 2D MR images of the *in vivo* normal hippocampal formation. Through these images, hippocampal sublayers are identified and reconstructed 3D structure of the normal canine hippocampal formation is obtained. The reconstructed hippocampal formation is superimposed on MR images. It would help in understanding the relationship of the hippocampal formation to other internal structures of the brain.

MATERIALS AND METHODS

Animals: The MRI scan was performed using 3 healthy beagle dogs ranging from 20 months to 25 months in age. An intact female and two intact males weighting 5–7 kg

* CORRESPONDENCE TO: EOM, K. D., Department of Veterinary Radiology and Diagnostic Imaging, College of Veterinary Medicine, Konkuk University, 1 Hwayang-dong, Kwangjin-ku, Seoul 143–701, Korea.
e-mail: eomkd@konkuk.ac.kr
**JUNG, M. A. and NAHM, S.-S. contributed equally to this work.

were used. They had no neurological signs related to brain dysfunctions on clinical exams. There were no remarkable findings on their MR images.

MRI acquisition and analysis: Dogs were scanned on 7T MR unit (Siemens MAGNETOM 7T magnet, German, From the Neuroscience Research Institute, Gachon University of Medicine and Science, Incheon 405–760, Korea) using T1-weighted 3D magnetization prepared rapid acquisition gradient echo (MPRAGE) sequence (Fig. 1). The MRI was performed while the dogs were in sternal recumbency and under general anesthesia with intravenous medetomidine hydrochloride (Domitor®, Pfizer Inc., Korea) and pentobarbital sodium (Entobar®, Hanlim Pharm, Korea). The bird cage type head coil was custom manufactured which was made to accommodate dog brain for this study. Measurement parameters were following: TR=2500 ms, TE=2.98 ms, TI=1100 ms, 6 averages, flip angle=10°, FOV=96 × 12, acquisition matrix=256 × 192, 128 dorsal slices, 0.5 mm slice thickness. The voxel size was 0.5 mm × 0.5 mm × 0.5 mm. MPRAGE scan acquisition time was approximately 16 min per dog. The scanned MRI data was transferred to the image analysis program and realigned in transverse and sagittal planes for review. All dogs were cared for in accordance with the guidelines for the care and use of laboratory animals approved by committee of Institutional Animal Care and Use Committee, Konkuk University.

3D model rendering and analysis: Open-access 3D slicer software (www.slicer.org, Artificial Intelligence Laboratory of Massachusetts Institute of Technology and Surgical Planning Laboratory at Brigham and Women's Hospital and Harvard Medical School) was employed for rendering and analyzing the 3D model. It carries out automatic volume conversion from original volume data, half-automatic image segmentation, produce 3D models of segmented structures, and 3D visualization.

In the present study, shape analysis was performed using the tracing of the left and right hippocampal formation. The 3D images were reconstructed from series of 2D slice-by-slice hippocampal segmentation based on previous human studies [6, 12, 19] and an atlas of the canine hippocampal anatomy [2]. The hippocampal proper, dentate gyrus, subiculum, alveus and fimbria were included in the boundary of the hippocampal formation [19].

First, the MRI data was transferred and reconstructed to produce the sagittal and transverse planar data from dorsal planar data. The 2D data were edited by threshold selection to improve the precision and reliability of the segmentation. The boundaries of the hippocampal formation were manually traced. The dorsal sectional images were mainly used to outline the boundaries of the hippocampal formation. However, because of the ambiguity between the gray matters of the hippocampal head and amygdale and the indistinct definition of the border of the hippocampal tail, the dorsal pane was combined with two other planar sections for tracing. The tracing proceeded dorsal to ventral with dorsal sectional images, cranial to caudal with transverse sectional images and lateral to medial with sagittal sectional images in a sequential method. The traced images of the hippocampal formation were labeled with a specific color. Algorisms were used to smooth noise and sharpen borders of labeled tissue. The labeled 2D slices were then put together automatically through the 3D slicer program to form a volume model of the hippocampal formation (Fig. 2).

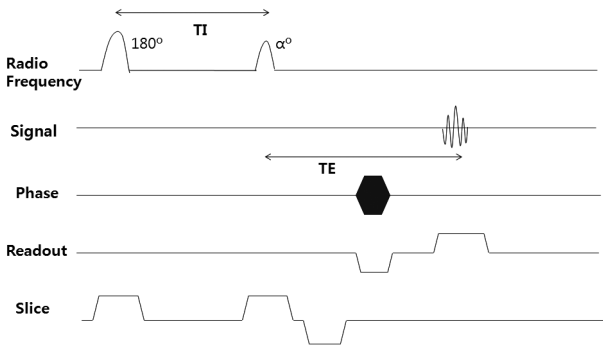

Fig. 1. Schematic diagram of the MPRAGE sequence. TI, time of inversion; TE, time of echo. This sequence has preparation time before α RF (Radio Frequency) pulse and 180° and/or 90° pulse is applied to the tissue to enhance the contrast [4, 20].

Automatically produced 3D image of the hippocampal formation showed on 3D window. This allowed reconstructed hippocampal formation to be observed from different angles. In addition, because the 3D window can also interact with three vertical sets of 2D plane windows, sectional MR images with different positions could be displayed. And then the relationship of the reconstructed hippocampal formation with surrounding structures was evaluated by superimposing MR images.

RESULTS

MPRAGE images: The hippocampal structure was obtained through the MPRAGE sequence. Especially, the subcomponent of the hippocampal formation including cornus ammonis, subiculum, alveus and fimbria were resolved. The hippocampal formation resembled a letter S on the dorsal and transverse sectional images, notably on the transverse sectional images. The dentate gyrus was interlocked with the hippocampal proper. The subiculum which had gray matter signal was continuous from the CA4 to the ventromedially. The alveus which showed white matter signal was converged to the fimbria on the dorsal part of the hippocampal formation (Fig. 3).

The ovoid shape of the hippocampal head was observed more clearly in the transverse sectional images than in the dorsal sectional images. On the transverse sectional images, the hippocampal head was delineated by the cerebrospinal fluid (CSF) in the ventral horn of the lateral ventricle. It was located dorsal to the parahippocampal gyrus and lay adjacent to the amygdala cranially. The hippocampal formation separated from the amygdala by thin layer of white matter,

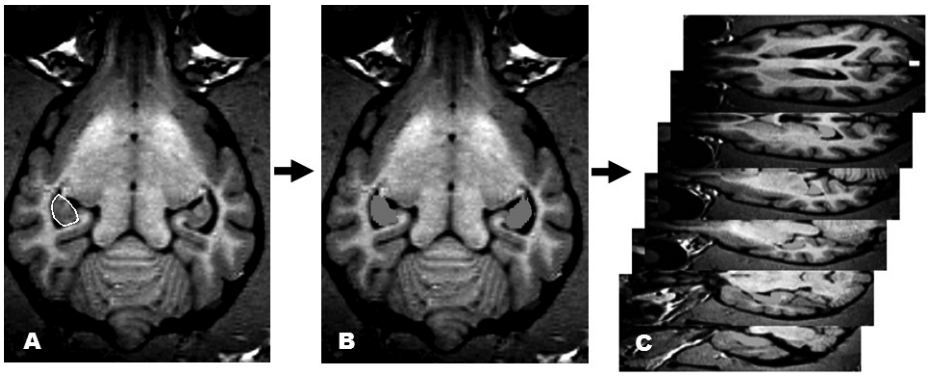

Fig. 2. The method of the three-dimensional model rendering. (A) Transferred MR data are edited by threshold selection and hippocampal formation was manually traced. Manually traced right hippocampal formation (white line) is shown on dorsal MR image. (B) Left hippocampal formation is also traced in same method and then the selected area was labeled with blue color. (C) Labeled two-dimensional slices were piled up together to produce three-dimensional hippocampal formation automatically through the 3D slicer program.

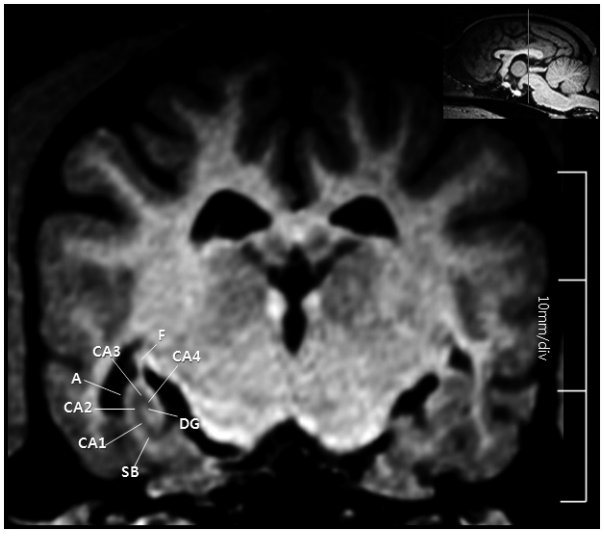

Fig. 3. Transverse MPRAGE image of the normal canine brain showing the hippocampal formation. The level of the image is indicated on the sagittal image, which has been inset into the image in the upper right corner of the image. This image is scanned in 256 × 192 and the actual resolution is 610 × 545 pixels. A, alveus; CA1–4, hippocampal proper; DG, dentate gyrus; F, fimbria; SB, subiculum. The bar is 30 mm.

alveus, was well visualized on the sagittal sectional images (Fig. 4).

The hippocampal body was most nicely visualized on the transverse and dorsal sectional images. It showed ovoid shaped mass in the lateral ventricle on the transverse sectional images. The lateral border of the hippocampal body was well delineated with respect to 2 other parts of the hippocampal formation because of the surrounding CSF in the lateral ventricle (Fig. 5).

The hippocampal tail appeared as ovoid gray matter ventromedial to the lateral ventricle. And the ventral margin of the hippocampal tail was demarcated by the CSF in the third ventricle ventral to the fornix on the transverse sectional images. The hippocampal tail with its characteristic gray matter was visualized most readily on the sagittal sectional images. It showed ovoid shape and was pointed cranially. The most cranial border of the hippocampal tail was delineated by the CSF in the dorsal horn of the lateral ventricle in the sagittal sectional images. The surface of the hippocampal tail was covered with alveus and it converged to the continuous white matter of fimbria (Fig. 6).

Three-dimensional hippocampal structure and surrounding anatomy: The overall contour of the hippocampal formation was in a C-shape but its cranial and caudal ends run medially (Fig. 7). The right and left halves of the hippocampal formation were divided into right and left cerebral hemispheres. They mirrored each other, as other cerebral structures. Hippocampal dorsal, middle and ventral part, which corresponds to tail, body and head respectively, were distinguishable. However, they merged into each other without distinct boundaries.

The 3D hippocampal formation showed how the boundaries relate to each other in different planes. The hippocampal head was observed caudal to the amygdala and dorsal to the parahippocampal gyrus. It lies virtually in transverse sectional images and continued to the hippocampal body caudodorsally. It was presented more cranially than the hippocampal tail (Fig. 8).

The middle part, hippocampal body made the largest portion of the hippocampal formation. The hippocampal body was found more dorsolaterally with respect to the hippocampal head and caudolaterally with respect to the hippocampal tail. The majority of the body encircled the caudolateral part of the thalamus, while they were separated by the temporal horn of the lateral ventricle (Fig. 9).

The hippocampal tail coursed caudally and curved medially to reach to the splenium of the corpus callosum. It

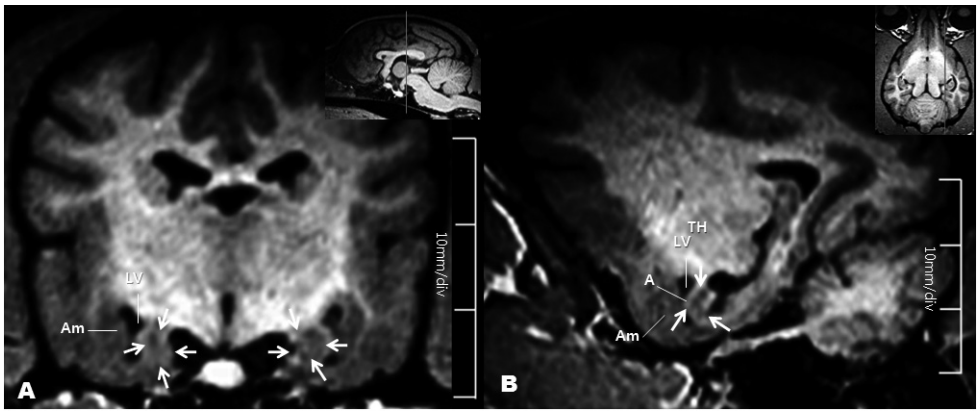

Fig. 4. Transverse and sagittal MPRAGE images of the normal canine brain at the level of the hippocampal head. Arrows show the hippocampal head. The level of the image is indicated on the sagittal and dorsal images, which has been inset into the image in the upper right corner of the images. Both images were scanned in 256 × 192 and the actual resolution of is 579 × 423 pixels (A) and 525 × 423 pixels. (A) The transverse sectional image showing the hippocampal head as small ovoid mass. (B) The hippocampal head is separated from the amygdale by the alveus. A, alveus; Am, amygdala; LV, lateral ventricle; TH, thalamus. The bars in A and B are 30 mm.

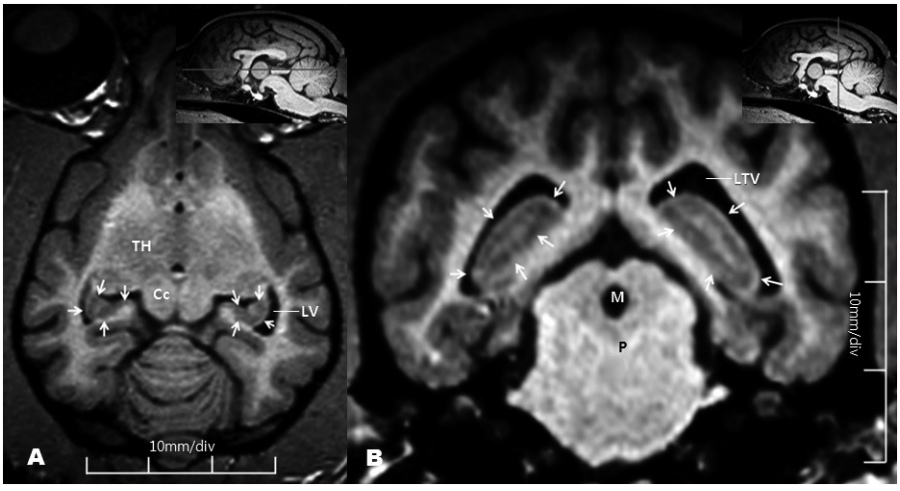

Fig. 5. Dorsal and transverse MPRAGE images of the normal canine brain at the level of the hippocampal body. Arrows show hippocampal body. The level of the image is indicated on the sagittal images, which has been inset into the image in the upper right corner of the images. Both images were scanned in 256 × 192 and the actual resolution of is 579 × 505 pixels (A) and 362 × 505 pixels (B). The hippocampal body is well delineated by the lateral ventricle on both images. Cc, caudal colliculus; LV, lateral ventricle; M, mesencephalic aqueduct TH; thalamus; P, pons. The bars in A and B are 30 mm.

showed dorsally convex arc bulging into the lateral ventricle forming the part of the medial wall of the lateral ventricle. It was located more caudal to the hippocampal head (Fig. 10).

DISCUSSION

In the present study, composite images of the normal living canine hippocampal formation were created. From these 3D structures, the *in vivo* anatomy of the hippocampal formation and its 3D relationships with the adjacent deep brain structures could be described.

Delineating hippocampal sublayers can be difficult without knowledge of the sublayer anatomy and signal characteristics of each component [10, 22]. High-resolution MPRAGE provide better defined gray, white matter and CSF differentiation compared with conventional 2D sequence [15]. As a result, MPRAGE at 7T demonstrated the major sublayers of the hippocampal formation: the alveus, fimbria, CA, dentate gyrus, subiculum, and parahippocampal gyrus. This made it easier to depict the hippocampal subcomponents; dentate gyrus, CA, subiculum, parahippocampal gyrus, alveus and fimbria, which was not

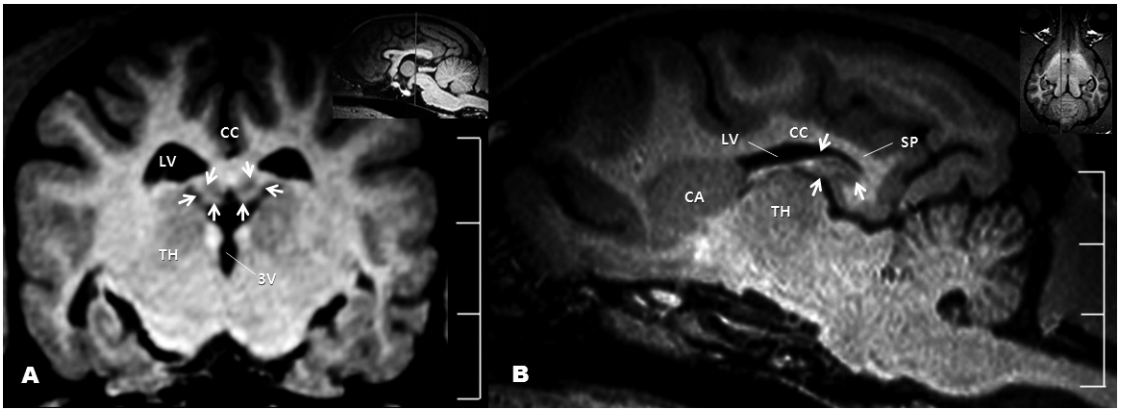

Fig. 6. Transverse and sagittal MPRAGE images of the normal canine brain at the level of the hippocampal tail. The level of the image is indicated on the sagittal images, which has been inset into the image in the upper right corner of the images. Both images were scanned in 256 × 192 and the actual resolution of is 482 × 422 pixels (A) and 663 × 422 pixels. (A) The hippocampal tail is delineated by the cerebrospinal fluid in the lateral ventricle and third ventricle on the transverse sectional image. (B) Hippocampal tail points cranially on the sagittal sectional image. 3V, third ventricle; CC, corpus callosum; CA, caudate nucleus; LV, lateral ventricle; SP, splenium of the corpus callosum; TH, thalamus. The bars in A and B are 30 mm.

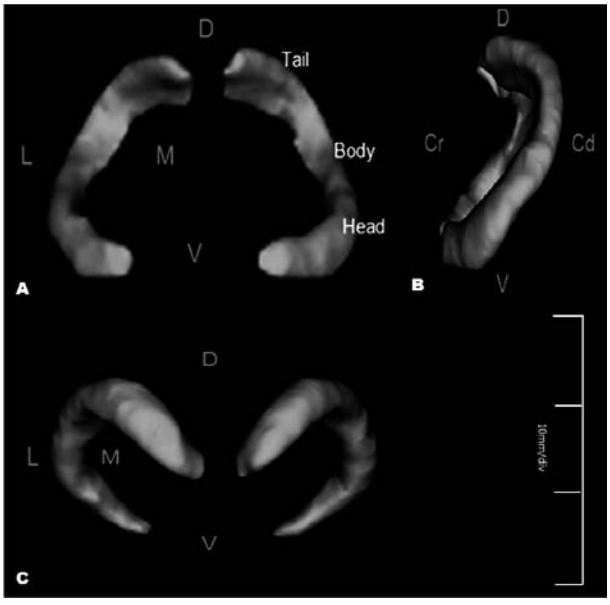

Fig. 7. Three-dimensional reconstructed images of the hippocampal formation. (A) Craniocaudal view. (B) Right lateral view. (C) Dorsoventral view. The right and left halves of the hippocampal formations face each other. The cranial and caudal hippocampal ends run medially, showing a "C" shape. D, dorsal; V, ventral; M, medial; L, lateral; Cr, cranial; Cd, caudal. The bars in A and B are 30 mm.

possible with a conventional 2D sequence. The layer with prominent gray matter signal is quite likely to be pyramidal cells in the CA, which is covered dorsally by the thin alveus showing white matter signal [19].

High-resolution MPRAGE allows 3D reconstruction due to near isotropy of the acquisition resolution. And it has capability to acquire very thin contiguous sections, minimizing problems with partial volume effects and intersection gaps that may lead to difficulty in visualization of small part particularly [15]. Thus, it was possible to acquire dorsal, transverse and sagittal images without any distortion making it possible tracing of the hippocampal formation on any planar images. Moreover, the increased signal to noise ratio, contrast and shorter image acquisition time make the 3D sequence a preferred source for the segmentation of the brain structures [15]. It also improves the visibility and detection of anatomical borders better than T1 weighted and T2 weighted of spin echo [3, 15, 19]. These advantages of MPRAGE sequence were taken to improve visualization and demarcation of the anatomical borders of the hippocampal formation. It was possible to detect the distinct borders between white matter and gray matter regions.

The canine hippocampal formation has been described as a horn shape. Its head, the most ventral part is lateroventrally convex and lie virtually in the transverse sectional planes. The hippocampal body has predominantly dorsoventral orientation, with its dorsal end more caudomedial than its ventral end and slightly lateral convexity. The hippocampal tail shows dorsally curving line rising above the corpus callosum and bulging into the lateral ventricle [21]. The gross shape of the 3D hippocampal formation was similar with the previous study. It had a "C" shaped contour and lateral convexity. The hippocampal head and tail run more medially than the hippocampal body. Bilateral hippocampal formation forms a commissure at the fornix, which is continuity of the fimbria, at the level of the splenium of the corpus callosum [1, 2]. However, in the present study, the fornix was not included when tracing, such that the bilateral hippocampal formation was divided into right and left cerebral hemispheres.

Very thin contiguous section of the MPRAGE minimizes spatial volume effect and interaction gaps [15]. As a result, it created a little errors and a contour closer to an actual hip-

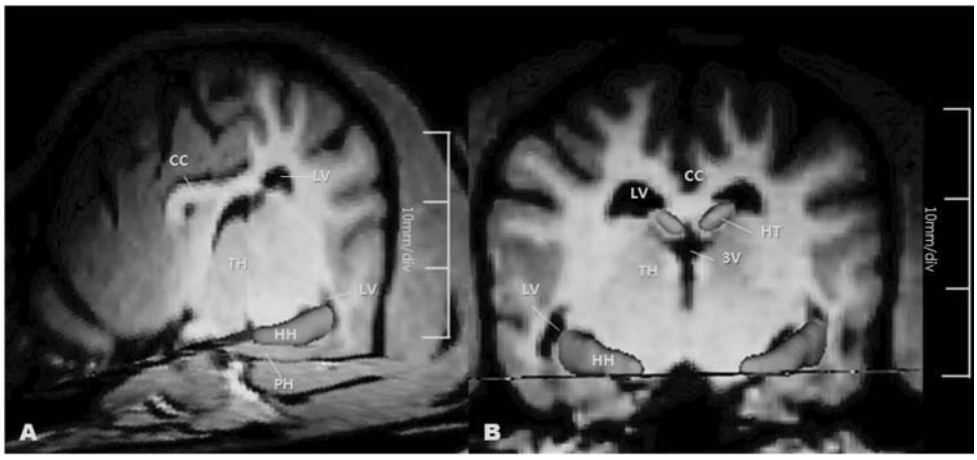

Fig. 8. Three-dimensional hippocampal formation superimposed on MR images mainly showing hippocampal head. (A) Sagittal, transverse and dorsal sectional images are combined to show the relationship of the hippocampal formation to surrounding structures. The hippocampal head is presented dorsal to the parahippocampal gyrus running caudodorsally. (B) Transverse and dorsal sectional images with hippocampal formation. The hippocampal head is present more cranially than hippocampal tail. And it lies in the temporal horn of the lateral ventricle. 3V, third ventricle; CC, corpus callosum; HH, hippocampal head; HT, hippocampal tail; LV, lateral ventricle; PH, parahippocampal gyrus.

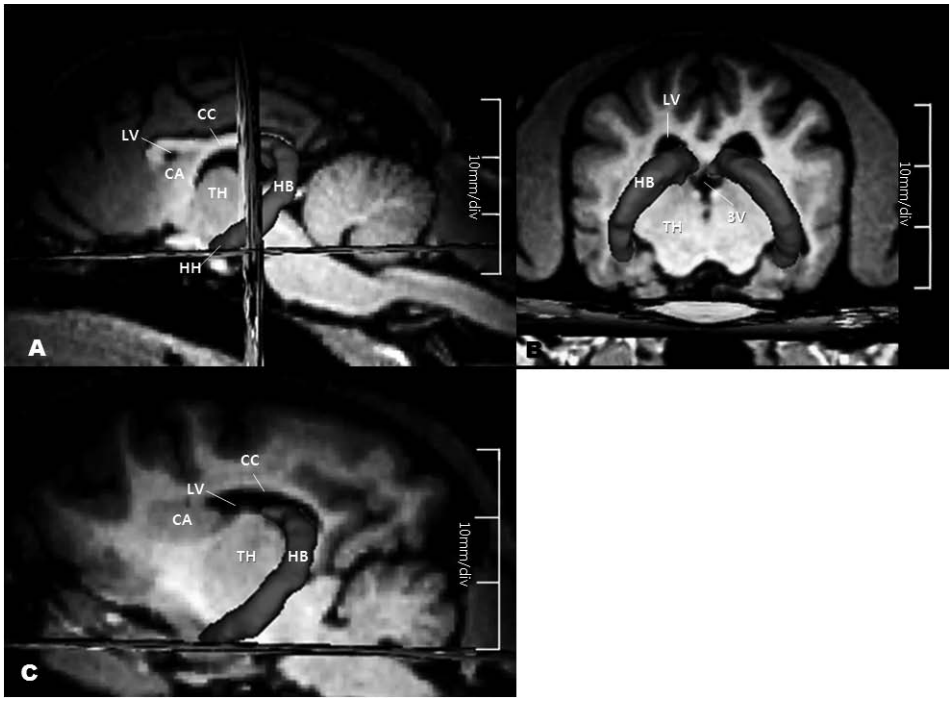

Fig. 9. Three-dimensional hippocampal formation superimposed on MR images prominently showing the hippocampal body. (A) Sagittal, transverse and dorsal sectional images are combined to show the relationship of the hippocampal formation to surrounding structures. The hippocampal body is presented in lateral direction and it runs caudodorsally from the hippocampal head. (B) Transverse and dorsal sectional images with the hippocampal formation. The hippocampal body has dorsoventral orientation and is vertical to the transverse sectional image. (C). Sagittal and dorsal sectional images with the hippocampal formation. Most part of the hippocampal body encircles the caudal part of the thalamus. 3V, third ventricle; CA, caudate nucleus; CC, corpus callosum; HB, hippocampal body; HH, hippocampal head; LV, lateral ventricle. The bars in A and B are 30 mm.

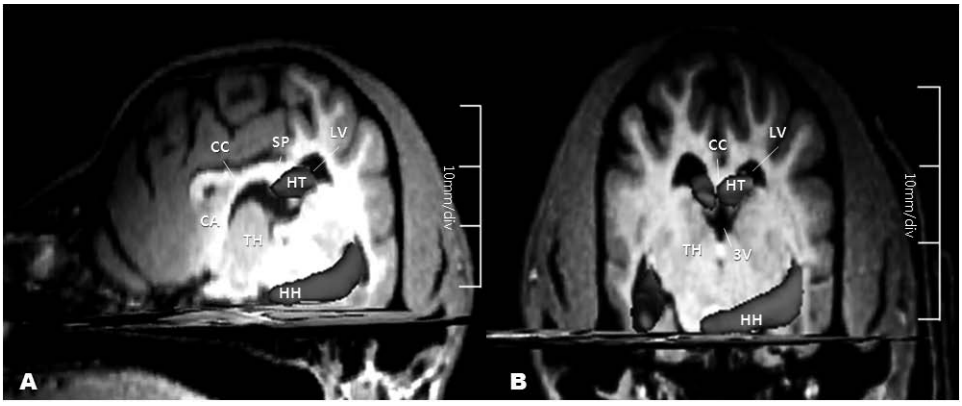

Fig. 10. Three-dimensional hippocampal formation superimposed with MR images showing hippocampal tail. (A) Sagittal and dorsal sectional images are combined to show the relationship of the hippocampal tail to surrounding structures. The hippocampal tail is situated ventral to the splenium of the corpus callosum and caudal to the thalamus. (B) Transverse and dorsal sectional images with the hippocampal formation. The hippocampal tail is presented more caudal than the hippocampal head. 3V, third ventricle; CA, caudate nucleus; CC, corpus callosum; HH, hippocampal head; HT, hippocampal tail; LV, lateral ventricle. The bars in A and B are 30 mm.

pocampal formation. However, the contour was not exactly same with the result of the previous report depicting the hippocampal formation from the dissected brain [21]. The deformed hippocampal formation in 3D structure did not have a tapered shape in the hippocampal tail. This disparity arises from technical differences in tracing the hippocampal formation on the MR images. In our study, the fornix was not taken into consideration and arbitrary lines were used to reconstruct hippocampal formation. It is likely that these methodological differences resulted in some difference between 3D structure using the MR image and histological morphology.

The hippocampal structure has been observed in 2D images allowing access to a surface of the structure at a time [1, 2, 21]. With this composite image, the structure could be accessed through the whole surface by the software in any direction. Furthermore, the hippocampal surface anatomy superimposed on the MR images assisted understanding the relationship of the hippocampal formation with other internal structures and appreciating its orientation in the brain.

The majority of protocols described manual tracing of hippocampal borders in human medicine [3, 5, 16, 19]. They usually used transverse sectional images and a few dorsal sectional images [3]. In the present study, all three orthogonal sectional images were used to depict anatomical boundaries of the hippocampal structure, while tracing was mainly performed in dorsal sectional images. It has been reported that the canine hippocampal formation has a similar position with respect to the sylvian fissure as in human; however, because the angle of the temporal lobe with respect to the remainder of the cerebrum differs, the canine hippocampal formation is oriented more vertical than that of human being [23]. This is supported by the fact that more slices were acquired in the dorsal sectional images in the canine hippocampal formation.

There are some limitations in this study. First, the sample size was not sufficient to demonstrate canine hippocampal formations from all breeds. Therefore, it is necessary to carry out a further study with larger sample from different breeds. Second, although the manual segmentation of brain structures for volume and shape analyses has provided actual volumes of structures, and allows more precise anatomical delineation of boundaries, it is time consuming and depends on experience with neuroanatomy [7, 9]. Therefore automated approaches will resolve these problems and facilitate analysis of data from larger scale studies [16].

The composite images were used to emphasize characteristic of normal hippocampal anatomy and to demonstrate the structural relationship of the hippocampal formation to surrounding structures *in vivo* on MR images. This is the first study that creates a 3D canine hippocampal formation model. The 3D hippocampal structure superimposed on MR images assisted in visualizing hippocampal formation in the various directions and in comprehending hippocampal orientation. The 3D hippocampal structure may be used as training material for neuroanatomy. It also will assist in comprehending hippocampal change on MR images for clinical use. It can be useful for early detection of hippocampal abnormalities showing progressive change. This may be a useful reference for quantitative analysis of the hippocampal formation in future studies of canine neurodegenerative diseases. Above all, it makes a way for further studies on the 3D structure of canine whole brain structures.

ACKNOWLEDGMENT. This work was supported by National Research Foundation of Korea Grant funded by the Korean Government. KRF-2008-A003-0061.

REFERENCES

1. Alexander, D. L. 2009. Nonolfactory rhinencephalone: Limbic system. pp. 448–453. *In*: Veterinary Neuroanatomy and Clinical Neurology, 3rd ed. St. Louis, Saunders.
2. Alvin, J. B. and Thomas, F. F. 1993. The brain. pp. 944–952. *In*: Miller's anatomy of the Dog, 3rd ed. (Howard E. E. ed.). Philadelphia, Saunders.
3. Bonilha, L. E., Kobayashi, Cendes, F. and Min, L. L. 2004. Protocol for volumetric segmentation of medial temporal structures using high-resolution 3-D magnetic resonance imaging. *Hum. Brain Mapp.* **22**: 145–154.
4. Donald, W. M., Elizabeth, A. M., Martin, J. G. and Martin, R. P. 2003. Acronums anomymous: a guide to the pulse sequence jungle. pp. 218–254. *In*: MRI from Picture to Proton. New York. Cambridge University Press.
5. Frisoni, G. B., Ganzola, R., Canu, E., Rüb, U., Pizzini, F. B., Alessandrini, F., Zoccatelli, G., Beltramello, A., Caltagirone, C. and Thompson, P. M. 2005. Mapping local hippocampal changes in Alzheimer's disease and normal ageing with MRI at 3 Tesla. *Brain* **131**: 3266–3276.
6. Geuze, E., Vermetten, E. and Bremner, J. D. 2005. MR-based *in vivo* hippocampal volumetrics: 1. Review of methodologies currently employed. *Mol. Psychiatry* **10**: 147–159.
7. Haller, J. W., Banerjee, A., Christensen, G. E., Gado, M., Joshi, S., Miller, M. I., Sheline, Y., Vannier, M. W. and Csernansky, J. G. 1997. Three-dimensional hippocampal MR morphometry with high-dimensional transformation of a neuroanatomic atlas. *Radiology* **202**: 504–510.
8. Henri, D. 2000. Brain anatomy. pp. 29–98. *In*: Magnetic Resonance in Epilepsy: Neuroimaging Techniques, 2nd ed. (Ruben I. K. and Graeme D. J. eds.). California, Elsevier.
9. Hsu, Y. Y., Schuff, N., Du, A. T., Mark, K., Zhu,X., Hardin, D. and Weiner, M. W. 2002. Comparison of automated and manual MRI volumetry of hippocampus in normal aging and dementiadementia. *J. Magn. Reson. Imaging* **16**: 305–310.
10. Jens, M. T., Kraff, O., Maderwald, S., Schlamann, M. U., Greiff, A., Forsting, M., Ladd, S. C., Ladd, M. E. and Gizewski, E. R. 2009. The Human hippocampal formation at 7T–*In Vivo* MRI. *Hippocampal Formation* **19**: 1–7.
11. Konrad, C., Ukas, T., Nebel, C., Arolt, V., Toga, A. W. and Narr, K. L. 2009. Defining the human hippocampus in cerebral magnetic resonance images – An overview of current segmentation protocols. *Neuroimage* **47**: 1185–1195.
12. Kowalska, D. M. 2000. Cognitive functions of the temporal lobe in the dog: a review. *Prog. Neuropsychopharmacol. Biol. Psychiatry* **24**: 855–880.
13. Kraft, S. L., Gavin, P. R., Wendling, L. R. and Reddy, V. K. 1989. Canine brain anatomy on magnetic resonance images. *Vet. Radiol. Ultrasound* **30**: 147–158.
14. Leigh, E. J., Mackillop, E., Robertson, I. D. and Hudson, L. C. 2008. Clinical anatomy of the canine brain using magnetic resonance imaging. *Vet. Radiol. Ultrasound* **49**: 113–121.
15. Michael, B. Z., Gillan, D., Olfgang, R. T. and Nitz, R. 1992. MPRAGE: A 3D, T1-weighted, gradient-echo sequence-initial experience. *Radiology* **182**: 769–775.
16. Morey, R. A., Petty, C. M., Xu, Y., Hayes, J. P., Wagner, H. R., Lewis, D. V., LaBar, K. S., Styner, M. and McCarthy, G. 2009. Comparison of automated segmentation and manual tracing for quantifying hippocampal and amygdala volumes. *Neuroimage* **45**: 855–866.
17. Narr, K. L., Thompson, P. M., Szeszko, P., Robinson, D., Jang, S., Woods, R. P., Kim, S., Hayashi, K. M., Asunction, D., Toga, A. W. and Bilder, R. M. 2004. Regional specificity of hippocampal volume reductions in first-episode schizophrenia. *Neuroimage* **21**: 1563–1575.
18. Posener, J. A., Wang, L., Price, J. L., Gado, M. H., Province, M. A., Miller, M. I., Babb, C. M. and Csernansky, J. G. 2003. High-dimensional mapping of the hippocampus in depression. *Am. J. Psychiatry* **160**: 83–89.
19. Pruessner, J. C., Li, L. M., Serles, W., Pruessner, M., Collins, D. L., Kabani, N., Lupien, S. and Evans, S. V. 2000. Volumetry of hippocampus and amygdala with high-resolution MRI and Three-dimensional analysis software: Minimizing the discrepancies between Laboratories. *Cereb. Cortex* **10**: 433–442.
20. Ray, H. H., William, G. B. and Christopher, J. L. 2004. Gradient echo: Part áU (Fast scanning techniques) pp. 252–262. *In*: MRI the Basics. Newyork. Lippincott Williams & Wilkins.
21. Salazar, I., Fernandez, T. P., Cifuentes, J. M. and Ruiz, P. P. 1991. Macroscopical and micoscopical anatomy of the hippocampus in the dog. *Biol. Struct. Morphog.* **3**: 45–52.
22. Thomas, B. P., Welch, E. B., Niederhauser, B. D., Whetsell, W. O., Anderson, A. W., Gore, J. C., Avison, M. J. and Creasy, J. L. 2008. High-resolution 7T MRI of the human hippocampal formation *in vivo*. *J. Magn. Reson. Imaging* **28**: 1266–1272.
23. Vullo, T., Narine, V. D., Stallmeyer, M. J., Gomez, D. G. and Cahill, P. T. 1996. Quantitation of normal canine hippocampus formation volume: correlation of MRI with gross histology. *Magn. Reson. Imaging* **14**: 657–562.
24. Walter, J. H. 2000. The Limbic system. pp. 202–238. *In*: Atlas of Functional Neuroamatomy, 2nd ed., Boca Ratom, Taylor and Francis.